

GENERATION OF SUPERLATTICE BANDSTRUCTURE USING A WAVEFUNCTION MATCHING TECHNIQUE

R. I. Taylor⁺, M. G. Burt^{*}, R. A. Abram⁺,
⁺ School of Engineering and Applied Science,
 University of Durham, Durham, DH1 3LE, U.K.
^{*} British Telecom Research Laboratories, Martlesham Heath,
 Ipswich, IP5 7RE, U.K.

(Received 18th August, 1986)

The bandstructure for complex wavevector for bulk semiconductors in the [100] and [111] directions has been calculated using a layer method - a technique that utilises empirical pseudopotentials. In addition to the usual Bloch type solutions, information is also obtained about the evanescent solutions. By using all these bulk solutions as a basis for the wavefunction in the superlattice, and by constraining the wavefunction to satisfy the relevant boundary conditions at the superlattice interfaces, the electronic bandstructure of the superlattice has been generated. This paper describes the method, and uses it to examine the electronic bandstructure of GaAs/AlAs superlattices in the [100] direction. In particular, the in-plane bandstructure of the superlattice conduction bands has been examined, as has the variation of the energy gap of the superlattice with AlAs mole fraction.

1. CALCULATION OF BULK BANDSTRUCTURE

The potential for a semi-infinite crystal is periodic in two dimensions, and so may be written as a two dimensional Fourier series

$$V(\underline{r}, z) = \sum_{\underline{g}} V(\underline{z}) \exp(i\underline{g} \cdot \underline{r}) \quad (1)$$

where \underline{r} is a position vector in the plane, z is the distance perpendicular to the plane and \underline{g} is a 2D reciprocal lattice vector.

Also, the two dimensional periodicity means that, by Bloch's theorem, a complete set of solutions to Schrodinger's equation can be written as

$$\Psi(\underline{r}, z) = \sum_{\underline{g}} \exp(i(\underline{k} + \underline{g}) \cdot \underline{r}) \Phi(\underline{z}) \quad (2)$$

where \underline{k} is the 2D reduced wavevector.

By substituting equations (1) and (2) into Schrodinger's equation (where $\hbar^2/2m = 1$), the following is obtained:

$$\left(-\frac{d^2}{dz^2} + (\underline{k} + \underline{g})^2 - E \right) \Phi(\underline{z}) = - \sum_{\underline{g}'} V_{\underline{g}-\underline{g}'}(\underline{z}) \Phi(\underline{z}) \quad (3)$$

For a given value of energy, and a given value of \underline{k} , the above equation may be solved to obtain $\Phi_{\underline{g}}(z)$ by modelling the potential using empirical pseudopotentials¹.

To obtain the bulk bandstructure for complex wavevector, the values of $\Phi_{\underline{g}}(z)$ at two different values of z separated by a monolayer are calculated numerically. The Bloch condition is then used to obtain the z component of the wavevector K_z . Hence, the E-K relationship is² obtained. This technique is known as the transfer matrix method^{2,3}. An example of a bulk bandstructure for complex wavevector is shown in figure (1) for GaAs in the [001] direction.

2. CALCULATION OF THE SUPERLATTICE BANDSTRUCTURE

Consider a superlattice consisting of alternate layers of materials A and B. To calculate the bandstructure of the superlattice, the wavefunction in semiconductor A is written as a linear

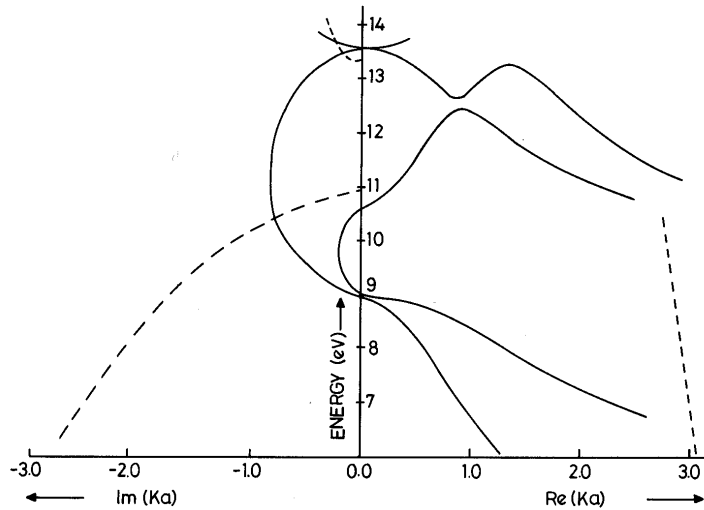


Figure 1 - The bandstructure for complex wavevector of GaAs in the [100] direction calculated using the transfer matrix method with $N=13$ and $ACCU=10E-3$. Solid lines correspond to either purely

real or purely imaginary wavevectors K , dashed lines correspond to complex wavevectors. (a = lattice constant of GaAs = 5.65\AA).

superposition of the A bulk basis states - these not only include the usual propagating Bloch states but also the evanescent states. Similarly, the superlattice wavefunction in semiconductor B is written as a linear superposition of the B bulk basis states. The problem is then to find the coefficients of the bulk basis states in the linear superposition. These coefficients are calculated by using the relevant boundary conditions at the semiconductor interface. The superlattice wavefunction and its derivative have to be continuous at the interfaces - since the complete Schrodinger equation has been solved, there are no ambiguities in the boundary conditions as occur in envelope function theories.

Also, the superlattice wavefunction (and its derivative) at z is related to the value at $(z + L)$ (where L is the superlattice period) by a superlattice Bloch condition. These constraints may be written as a matrix equation, and it is found that, if K_s is the superlattice wavevector, then $\exp(-iK_s L)$ is an eigen

value of the matrix $M_1^{-1} M_2 Q_B^{-S} M_2^{-1} M_1 Q_A^{-T}$. M_1 & Q_A are square matrices containing information about the properties semiconductor A, and M_2 & Q_B are the corresponding matrices for semiconductor B. S = The number of monolayers of semiconductor B in the B layers of the superlattice. T = corresponding number of monolayers for semiconductor A.

The dimensions for the square matrices above depend on the number of surface reciprocal lattice vectors used to calculate the bulk bandstructure. If N surface reciprocal lattice vectors are used, then the square matrices have dimension $2N$. The typical size of the matrices used is 26×26 . The matrix manipulation and diagonalisation of matrices of these dimensions was carried out rapidly using a mainframe computer.

Since empirical pseudopotentials are used, it is straightforward to look at a variety of superlattice systems. Here the method is restricted to lattice matched semiconductors. However, it is possible to use the technique for

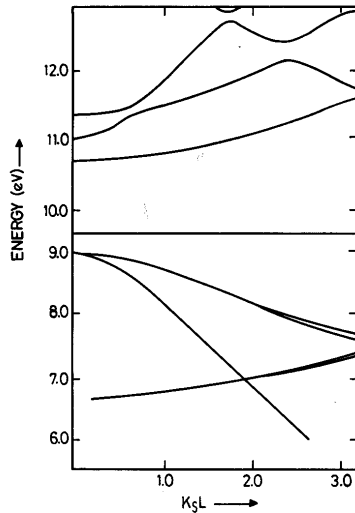


FIGURE 2(a)

Figure 2 - The energy-superlattice wavevector dispersion relation for a $(\text{GaAs})_9(\text{AlAs})_1$ superlattice. $N=9$, $\text{ACCU}=10\text{E}-3$ and $\underline{k}=(0,0)$. Figure 2(a) has

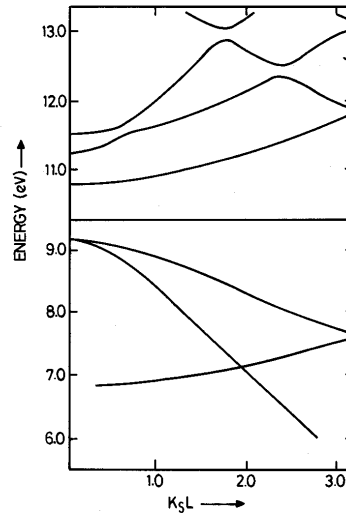


FIGURE 2(b)

a 60:40 ratio of conduction to valence band discontinuities and figure 2(b) has an 85:15 ratio. (L is the superlattice period).

strained layer systems and this will be discussed in a future publication.

The conduction and valence band discontinuities may also be varied by rigidly shifting the bandstructure of one of the constituent semiconductors upwards or downwards in energy. Hence, the latest values of band offsets may be incorporated into the program.

The bandstructure of the superlattice in the plane parallel to the interfaces may be examined by calculating the bulk bandstructure with a non-zero value of \underline{k} . If a scan through the energy range is performed to find a fixed value of K_x , (e.g. $K_x = 0.0$) then the $E-k$ dispersion relations may be obtained for a particular, fixed, value of K_x . This information is important for calculations of Auger recombination rates⁵, carrier transport etc.

Finally, we note that quantum well bandstructure may also be obtained by simply letting the barrier thickness become very large.

3. RESULTS

To demonstrate the feasibility of our method for the calculation of superlattice bandstructure, the AlAs/GaAs superlattice has been examined in the [100] direction. Spin-orbit splitting has been omitted from this preliminary calculation but can be included without difficulty.

The accuracy of our calculation is determined by two quantities:

- (a) N - the number of surface reciprocal lattice vectors used to generate the bulk bandstructure for complex wavevector.
- (b) ACCU - a parameter that is used in the numerical routine for solving equation (3) of section 1.

For high accuracy (large N and small ACCU) it is necessary to use a large amount of computer time, which can only be decreased by compromising the accuracy.

In figure (2), the energy-superlattice wavevector dispersion relationship has been plotted

for the ultimate short period superlattice - one monolayer of GaAs alternating with one monolayer of AlAs. In calculating the results for figure (2), nine surface reciprocal lattice vectors were used to generate the bulk bandstructure, and $ACCU=10E-3$, and the in-plane wavevector was chosen to be zero. Figure 2(a) shows the results when a 60:40 ratio of the direct conduction band discontinuity to the valence band discontinuity is used, whereas figure 2(b) has used an 85:15 ratio. In the figure, K_{\parallel} is the superlattice wavevector and S_L is the superlattice period, which, in this case is twice the period of the bulk semiconductors used. This means that the Brillouin-zone edge for the superlattice is half that of the bulk value, and the zone-folding effect can be clearly seen in the bands in the figure.

For the monolayer AlAs/GaAs superlattice, the dispersion of the conduction subbands in the plane parallel to the superlattice layers has also been examined. In figure (3) the in-plane dispersion relation for a $\langle 100 \rangle$ direction is illustrated. Figure 3(a) assumes a 60:40 ratio of the conduction and valence band discontinuities whereas figure 3(b) has used an 85:15 ratio. For all points in figure (3) the superlattice wavevector is zero. Only the conduction band in-plane dispersion relations have been shown since, with the absence of spin-orbit splitting, any in-plane dispersion relations for the valence band will be inaccurate.

The variation of energy gap with mole fraction of AlAs can be examined by simply looking at the energy gap of the superlattice for various well and barrier widths. The results of this calculation are illustrated in figure (4). In this figure, the crosses are results for a set of superlattices where the period changed by a monolayer at a time. For example, a 50% AlAs mole fraction corresponds to a $(AlAs)_1(GaAs)_1$ superlattice, whilst a 10% AlAs mole fraction corresponds to a $(AlAs)_1(GaAs)_9$ superlattice and a 90% mole fraction is $(AlAs)_9(GaAs)_1$. The circles illustrate the case of a superlattice where the period is changed by two monolayers at a time. The results show that there is a steep rise in the energy gap for low AlAs mole fractions - this is the direct gap regime, whereas at high AlAs mole fractions, the change in energy gap is not so steep - this is the indirect gap regime. The results are similar to the energy gap - mole fraction variation in a AlGaAs alloy⁶, however, it must be

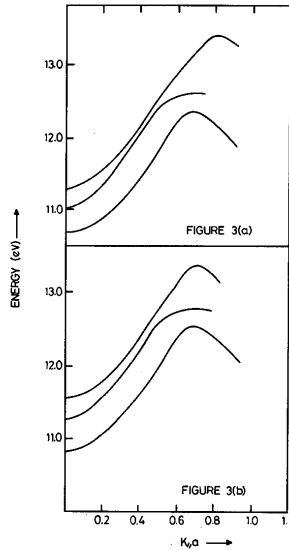


Figure 3 - The energy - in-plane wavevector dispersion relation for a $(GaAs)_1 (AlAs)_1$ superlattice in a $\langle 100 \rangle$ direction. $N=9$, $ACCU=10E-3$ and $K_{\parallel}=0.0$. Figure 3(a) has a 60:40 ratio, and figure 3(b) has an 85:15 ratio of conduction to valence band discontinuities. (a = lattice constant of GaAs, $AlAs = 5.65\text{\AA}$).

remembered that only thin superlattices have been examined. For wider wells (i.e. wider layers of GaAs) it is expected that the energy gap at large AlAs molefractions should tend towards the quantum well bandgap. This is consistent with our results, since, at high AlAs mole fractions, the energy gap in the wider well superlattice is smaller than that for the narrower wells.

4. SUMMARY

The transfer matrix method for the calculation of bulk bandstructure for complex wavevector for semiconductors has been described. Using a wavefunction matching technique, the bulk bandstructure has been used to generate the bandstructure of a superlattice. Empirical pseudopotentials have been used and so in addition to

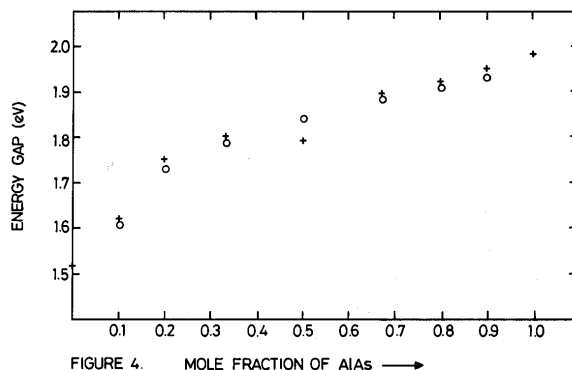


FIGURE 4. MOLE FRACTION OF AlAs →

Figure 4 - The zero temperature energy gap of two different types of superlattice versus mole fraction of

AlAs. See text for explanation. $N=21$, $ACCU=10E-4$, and $\underline{k}=(0,0)$

changing well and barrier widths, the well and barrier materials may also be changed without difficulty. At present, our technique has only been applied to lattice matched materials, but extension of our work to lattice mismatched materials will be discussed in a later paper. Our method has been used to calculate E-K dispersion relations for AlAs/GaAs superlattices in the [100] direction, and also to examine the in-plane dispersion relations in these superlattices. In addition, the energy gap of this superlattice has been examined as a function of AlAs mole fraction.

Acknowledgements

The authors would like to thank Drs. S. Brand, S. Monaghan, C. Smith, M. J. Adams and Mr. D. T. Hughes for useful discussions. They would also like to thank Drs. N. J. Doran and K. J. Blow for the use of computing facilities at BTRL. RIT acknowledges tenure of a UK

SERC CASE award in association with British Telecom Research Laboratories and the authors are grateful to the Director of Research at British Telecom for permission to publish this work.

References

1. A. Baldereschi, E. Hess, K. Maschke, H. Neumann, K-R Schulze, and K. Unger, *J. Phys. C: Solid St. Phys.*, **10**, 4709-4717 (1977).
2. M. G. Burt and J. C. Inkson, *J. Phys. D: Appl. Phys.*, **9**, 43-53 (1976).
3. M. G. Burt, *J. Phys. C: Solid St. Phys.*, **13**, 1825-1834, (1980).
4. J. Batey and S. L. Wright, *J. Appl. Phys.*, **59**, 200-209, (1986).
5. R. I. Taylor, R. A. Abram, M. G. Burt and C. Smith, *IEE Proc.*, **132**, Part J, 364-370 (1985).
6. Landolt-Börnstein series, III-V Data book, volume 17(a), 604. Published by Springer-Verlag Berlin.